Available online at www.sciencedirect.com
ScienceDirect
Ceramics International 35 (2009) 1569–1574
CERAMICS INTERNATIONAL
www.elsevier.com/locate/ceramint

Effect of the addition ZrO_2–Al_2O_3 on nanocrystalline hydroxyapatite bending strength and fracture toughness

I. Mobasherpour [a,*], M. Solati Hashjin [b], S.S. Razavi Toosi [a], R. Darvishi Kamachali [a]

[a] *Ceramics Department, Materials and Energy Research Center, P.O. Box 31787-316, Karaj, Tehran, Iran*
[b] *Medical Engineering Department, Amirkabir University, Tehran, Iran*

Received 3 June 2008; received in revised form 27 July 2008; accepted 27 August 2008
Available online 1 October 2008

Abstract

Nanocrystalline hydroxyapatite powder has been synthesized from a $Ca(NO_3)_2{\cdot}4H_2O$ and $(NH_4)_2HPO_4$ solution by the precipitation method. In the next step we prepared ZrO_2–Al_2O_3 powder. After preparation, the powder was dried at 80 °C and calcined at 1200 °C for 1 h. Various amounts (HAP–15 wt% ZA, HAP–30 wt% ZA) of powder were mixed with the hydroxyapatite by ball milling. The powder mixtures were pressed and sintered at 1000 °C, 1100 °C and 1200 °C for 1 h. In order to study the structural evolution, X-ray diffraction (XRD) was used. Transmission electron microscopy (TEM) and scanning electron microscopy (SEM) were used to estimate the particle size of the powder and observe fracture surfaces. Results show that the bending strength of pressed nanocrystalline HAP was improved significantly by the addition 15 wt% of ZrO_2–Al_2O_3 powders at 1200 °C, but the fracture toughness was not changed, however when 30 wt% of ZA powders were added to nanocrystalline HAP, the bending strength and fracture toughness of the specimens decreased at all sintering temperature.

Keywords: Nanocrystalline hydroxyapatite; Zirconia–Alumina (ZA); Bending strength; Fracture toughness

1. Introduction

Hydroxyapatite (HAP: $Ca_{10}(PO_4)_6(OH)_2$) has attracted much attention as a substitute material for damaged teeth or bones over the past several decades because of its crystallographical and chemical similarity with various calcified tissues of vertebrates [1–3]. The principal limitation of this material is that it is brittle and weak, which restricts the clinical orthopedic and dental applications [4,5].

There are several approaches for the improvement in mechanical properties of the HAP. One is to fabricate HAP reinforced with other ceramics. This approach has attracted much attention since the successful development of ceramic–matrix composite materials [6].

To be effective as a reinforcing agent for a ceramic–matrix composite material, the following conditions should be satisfied. First, the strength of the second phase must be higher than that of the matrix. Second, the interfacial strength between the matrix and the second phase should be neither too weak nor too strong. For an appropriate interfacial strength, no excessive reaction should occur between the matrix and second phase. In addition, the coefficient of thermal expansion (CTE) of the second phase should not differ too much from that of the matrix [7]. In the case of biomaterials, the biocompatibility of the reinforcing agent is another important factor that should be considered [8].

Zirconia has been commonly used as reinforcement for many ceramics because of its high strength and fracture toughness [9,10]. Bioinertness is another merit of the ZrO_2 [11]. However, extensive reaction between the HAP and the ZrO_2 to from TCP and fully stabilized ZrO_2 is a serious disadvantage of this approach [12,13].

Alumina, which is also classified as a bioinert material, has been widely investigated as a reinforcing agent for HAP [14]. Therefore, it is desirable to combine the advantages of both materials as reinforcements for the HAP: the excellent mechanical properties of ZrO_2 and the chemical inertness of Al_2O_3 with respect to HAP. ZrO_2–Al_2O_3 is one possible approach.

* Corresponding author. Tel.: +98 261 6204131.
E-mail address: I_mobasherpour@merc.ac.ir (I. Mobasherpour).

0272-8842/$34.00
doi:10.1016/j.ceramint.2008.08.017

In this work, the precipitation method has been adapted to synthesize nanocrystalline HAP and we investigated the effects calcined of powder of ZrO_2–Al_2O_3 on the mechanical properties of nanocrystalline HAP powder. The powder was done by a colloidal process utilizing electrostatic force between the ZrO_2-sol and the Al_2O_3 precursor, AlOOH. The morphology of nanocrystalline HAP powder and final powder of ZrO_2–Al_2O_3 after being calcined were observed by TEM. After densification, the mechanical properties, the relative proportion of TCP formed, the microstructures of the composite, and the fracture surface were observed.

2. Experimental

Nanocrystalline hydroxyapatite compounds were prepared by a solution-precipitation method using $Ca(NO_3)_2{\cdot}4H_2O$ (Analar No. 10305) and $(NH_4)_2HPO_4$ (Merck No. 1205) as starting materials and ammonia solution as agents for pH adjustment. A suspension of 0.24 M $Ca(NO_3)_2{\cdot}4H_2O$ was vigorously stirred and its temperature was maintained at 25 °C. A solution of 0.29 M $(NH_4)_2HPO_4$ was slowly added dropwise to the $Ca(NO_3)_2{\cdot}4H_2O$ solution. In all experiments the pH of $Ca(NO_3)_2{\cdot}4H_2O$ solution by ammonia solution was 11. The precipitin HAP was removed from solution by the centrifuge method at a rotation speed of 3000 rpm. The resulting powder was dried at 100 °C.

In the next step, $AlCl_3{\cdot}6H_2O$ (Merck No. 1084) and $ZrOCl_2{\cdot}8H_2O$ (Merck No. 8917) were used as the starting materials for preparation of ZrO_2–Al_2O_3. The pH of the suspensions was controlled by using 0.01N HCl solution as an acid. First, the optimal pH required for change of aluminum chloride to a gel containing bohmite (AlOOH) was estimated because bohmite is generated by hydrolyzing aluminum chloride in an acidic medium. The sol containing zirconium hydroxide from zirconium chloride (which was prepared in an acid medium by hydrolyzing) was added to alumina base gel. The resulting mixture was heated for 12 h in a drier at the temperature of 80 °C and then calcined at 1200 °C for 1 h. The name of the resulting powder is ZA powder. ZrO_2:Al_2O_3 ratio is 1 in ZA powder. To obtain this ratio, starting materials including $AlCl_3{\cdot}6H_2O$ and $ZrOCl_2{\cdot}8H_2O$ were weighted according to their ratios in Eqs. (1) and (2).

Various amounts of ZA powder were mixed with the nanocrystalline HAP by ball milling in distilled water for 24 h with Al_2O_3 balls as media to break the HAP agglomerates. The powder mixtures were pressed in a steel mold at room temperature with an applied pressure of 500 kg. The dimensions of the pressed sample were 4 mm × 6 mm × 40 mm. Sintering conditions for pure hydroxyapatite specimens was identical to sintering condition for composites specimens that is, sintering in 1000 °C, 1100 °C and 1200 °C for 1 h.

The phase transformation of the ZA powder and pressed bodies were determined with an X-ray diffractometer (Siemens, 30 kV and 25 mA) with Cu Kα radiation (λ = 1.5405 Å).

Transmission electron microscopy (TEM) was used to characterize the particles of HAP and ZrO_2–Al_2O_3. For this purpose, particles were deposited onto Cu grids, which support a "holey" carbon film. The particles were deposited onto the support grids by deposition from a dilute suspension in acetone or ethanol. The particle shapes and sizes were characterized by diffraction (amplitude) contrast and, for crystalline materials, by high resolution (phase contrast) imaging.

Bending strengths were measured at room temperature in air with a crosshead speed of 0.5 mm/min by three-point bending test. Test specimens with dimensions of 3.5 mm × 5 mm × 35 mm were cut and machined for bending strength and fracture toughness tests. The entire specimen surface was ground with an 800-grit diamond wheel and the tensile surface was polished with diamond slurries. The fracture toughness was determined by the indentation-strength method using an applied load of 500 N. For each set of conditions, at least five specimens were tested for both the strength and the fracture toughness measurements.

The fracture surfaces were observed with a Cambridge scanning electron microscope (SEM) operating at 25 kV.

3. Results and discussion

3.1. Synthesis nanocrystalline hydroxyapatite powder

The XRD peaks for hydroxyapatite powder after drying are illustrated in Fig. 1(a). The crystal phase of precipitated HAP powder before calcinations and after drying at 100 °C was all HAP. It contains no other crystalline phase other than HAP. The broad patterns around at (2 1 1) and (0 0 2) indicate that the crystallites are very tiny in nature with much atomic oscillations. TEM micrographs of the HAP powders before sintering and after drying are seen in Fig. 2. The microstructure of the HAP particles after drying is observed be almost like needle shape, with particle size in the range 8–20 nm. Results show that HAP nanocrystalline can successfully be produced by precipitation technique from raw materials.

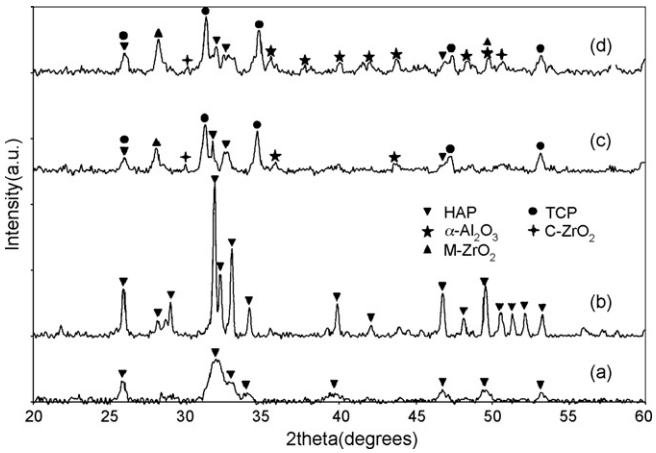

Fig. 1. XRD patterns of (a) nanocrystalline hydroxyapatite powders after drying at 100 °C, (b) nanocrystalline hydroxyapatite powders after calcinated at 1200 °C and (c), (d) HAP with 15 wt% ZA and HAP with 30 wt% ZA, respectively, after pressing and sintering.

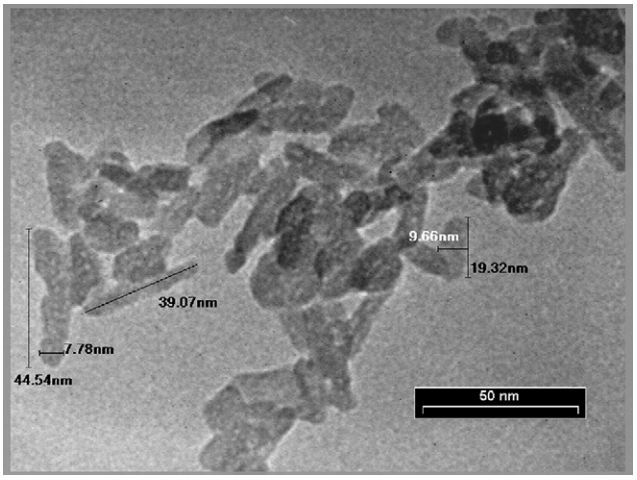

Fig. 2. TEM micrograph of the nanocrystalline hydroxyapatite after drying at 100 °C.

3.2. Synthesis ZrO_2–Al_2O_3 composite powder

The ZrO_2–Al_2O_3 mixture precursor is dried and then under gone the phase analysis, in Fig. 3(a) the pattern of XRD this stage is seen. As indicated in the patterns, the peaks of starting materials $AlCl_3.6H_2O$ and bohmite phase are recognizable. This indicates that bohmite gel exists beside that stating material $AlCl_3{\cdot}6H_2O$. As a result, when the hydrated chloride of aluminum is hydrolyzed, AlOOH phase is formed, and from among the aluminum hydroxides only AlOOH is changed into a transparent gel. In Fig. 3(b) diffraction pattern, the ZrO_2–Al_2O_3 mixture precursor after calcinated is seen. Considering this pattern the starting dried phases has been change into alumina and zirconia phase after being calcinated at 1200 °C, and phases α-alumina and monoclinic zirconia are easily recognizable beside each other. As sol–gel processing is based on several chemical processes such as hydrolysis and polycondensation, this need to be further considered.

In this case hydrolysis can take place by any of the following equations for alumina and zirconia precursor, respectively [15]:

$$AlCl_3 + 2H_2O \leftrightarrow AlOOH + 3H^+ + 3Cl^- \quad (1)$$

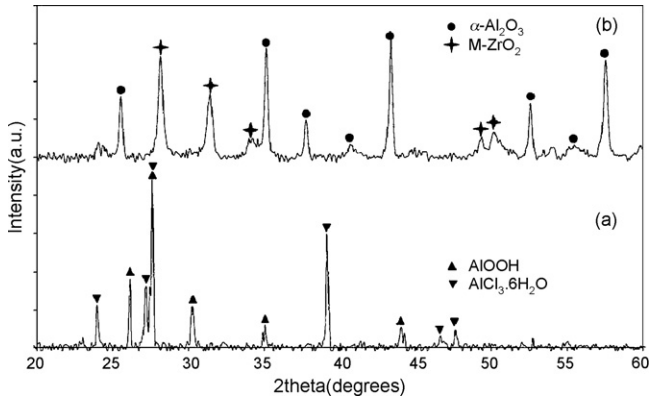

Fig. 3. XRD profiles of (a) ZrO_2–Al_2O_3 mixture precursor after drying at 80 °C for 12 h and (b) ZrO_2–Al_2O_3 mixture precursor after calcinated at 1200 °C for 1 h.

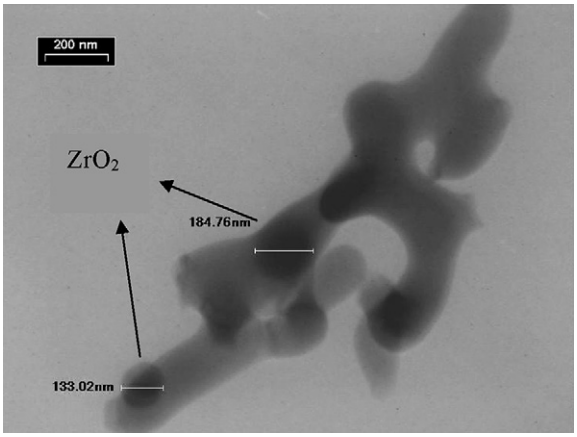

Fig. 4. TEM image of ZrO_2–Al_2O_3 mixture precursor after calcinated at 1200 °C for 1 h.

$$ZrOCl_2 + 2H_2O \leftrightarrow ZrO(OH)_2 + 2H^+ + 2Cl^- \quad (2)$$

The phase transition for zirconia and alumina by the heating from XRD is

$$ZrO(OH)_2 \rightarrow \text{m-}ZrO_2$$

$$AlOOH \rightarrow \alpha\text{-}Al_2O_3$$

The zirconia precursor powder is amorphous before calcinations, and shows monoclinic structure after calcinated [13].

TEM image of ZrO_2–Al_2O_3 after calcinated is seen in Fig. 4. All of the particles were composed of 300–500 nm clusters, which contained zirconia whose size was about 100–200 nm, as shown in Fig. 4. Since a greater number of nucleation sites were formed in the gel as the polymer content increased, the zirconia gradually grew into particles and eventually become a composite powder through their merging with alumina [16].

3.3. Mechanical properties

Fig. 5 shows the strength and fracture toughness of pure HAP and HAP/Al_2O_3–ZrO_2 composite as a function of sintering temperature. In all mechanically tested, the strength increased as the sintering temperature elevated. The strength of the pure HAP, HA–15ZA and HA–30ZA samples sintered at 1000 °C and 1200 °C was about 18 MPa, 30 MPa, 12 MPa and 38 MPa, 91 MPa, 23 MPa, respectively. The strength of the bodies sintered at 1000 °C was too low due to the insufficiently high sintering temperature. However, as the sintering temperature increased to 1200 °C, the strength value increased. Also, the fracture toughness does not significantly change as the sintering temperature increases. The fracture toughness of the pure HAP, HA–15ZA and HA–30ZA samples sintered at 1000 °C and 1200 °C was about 0.82 MPa $m^{0.5}$, 0.78 MPa $m^{0.5}$, 0.24 MPa $m^{0.5}$ and 1 MPa $m^{0.5}$, 0.9 MPa $m^{0.5}$, 0.25 MPa $m^{0.5}$, respectively. Therefore, the samples which sintered at 1200 °C were selected for a set of structural examinations, due their superior strength and toughness. Considering the decomposition of HAP to TCP at over 1400 °C and creation of large pores, this temperature (1200 °C) was selected as the final stage.

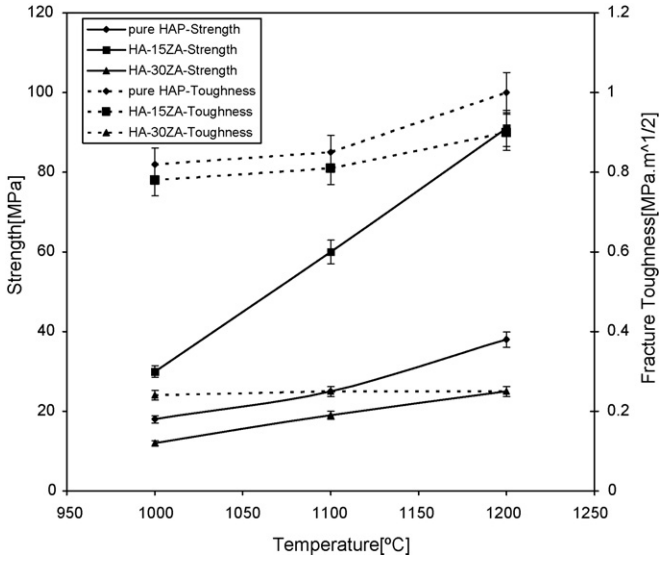

Fig. 5. Strength and fracture toughness of pure HAP, HA–15ZA and HA–30ZA depending on sintering temperature.

After pressing and sintering, the composition of the specimens sintered at 1200 °C was analyzed by means of their XRD patterns. Representative XRD patterns of the HAP-based composites are shown in Fig. 1(b–d). When pure HAP was pressed, and sintered at 1200 °C, only peaks corresponding to HAP were detected, as shown in Fig. 1(b). When 15 wt% ZA and 30 wt% ZA powder were added and sintered under the same condition, stronger TCP peaks were detected along with monoclinic zirconia, cubic zirconia, α-alumina and HAP peaks as seen in Fig. 1(c and d), the peaks of TCP due to the reaction between HAP and ZrO_2 [16]. The degree of reaction between the HAP and the second phases was estimated from the amounts of TCP generated (Fig. 6). The relative amount of TCP to HAP was deduced from the intensities of HAP peaks and TCP peaks. By the XRD analyses alone, it is hard to determine the precise amounts of phases present in a specimen. It is still useful in distinguishing the relative differences between the specimens processed under the same conditions. When 15 wt% ZA was added, the amount of TCP was less than the case of 30 wt% ZA addition, indicating extensive reaction between the HAP and the ZrO_2 to form TCP and cubic ZrO_2 as follows [13]:

$$Ca_{10}(PO_4)_6(OH)_2 \leftrightarrow 3Ca_3P_2O_8 + CaO + H_2O \quad (3)$$

$$CaO + ZrO_2 \leftrightarrow \text{cubic-}ZrO_2 \text{or} CaZrO_3 \quad (4)$$

From reaction (3), hydroxyapatite transforms into TCP together with releasing calcium (or CaO) and evolving water vapor. HAP phase is not stable, and TCP are the major phase. According to reaction (4), the reaction continues, a lot of CaO is released, thus cubic-ZrO_2 are formed. Also results of the XRD profiles shows, at the temperature sintering of 1200 °C, it is confirmed that the peaks of HAP, TCP, α-Al_2O_3, m-ZrO_2 and c-ZrO_2 phases were detected without the formation of any calcium aluminates phases such as $Ca_3Al_2O_6$, $CaAl_2O_4$, $CaAl_4O_7$, and $CaAl_{12}O_{19}$. The calcium aluminates peaks were detected as a minor reaction phases at the higher temperature sintering [17].

The effects of second phases on the mechanical properties of the HAP are shown in Figs. 7 and 8. The bending strength and fracture toughness of the pure HAP are about 38 MPa and 1 MPa $m^{0.5}$, respectively. When 15 wt% ZA was added to the HAP under the same condition, the bending strength increased to about 91 MPa, while the fracture toughness remained about the same. This improvement is believed to be closely related to the presence of the ZrO_2–Al_2O_3 particles preserved in the HAP matrix. The effectiveness of 15 wt% ZA in improving the bending strength of the HAP is well illustrated by these results. With further increase in the quantity of ZA particles, both the bending strength and the fracture toughness decreased, apparently due to the excessive reaction between the HAP and the ZrO_2 to form the TCP and cubic-ZrO_2 as mentioned above. The main factor affecting the reaction is the contact area between HAP and zirconia. In this study, the use of 15 wt% ZA powder was thought to decrease the contact area between HAP and zirconia, which would hinder the reaction, but the use of 30 wt% ZA powder was thought to increase the contact area, consequently indicating extensive reaction between the HAP and M-ZrO_2.

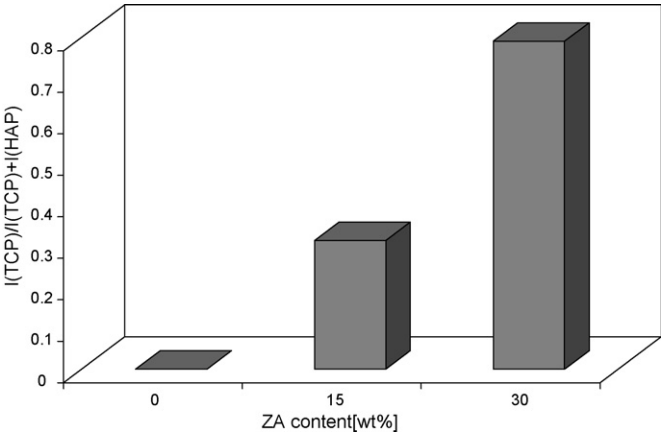

Fig. 6. Relative amounts of TCP to HAP deduced from the XRD patterns, indicating the degree of decomposition reaction between the HAP and the second phases.

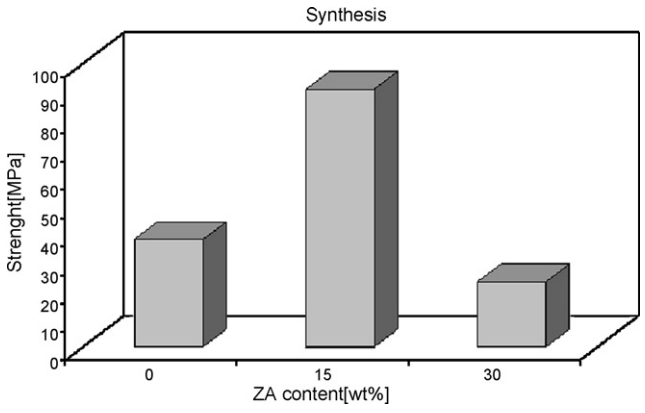

Fig. 7. Bending strength of the HAP-based composites containing various types of second phases at 1200 °C.

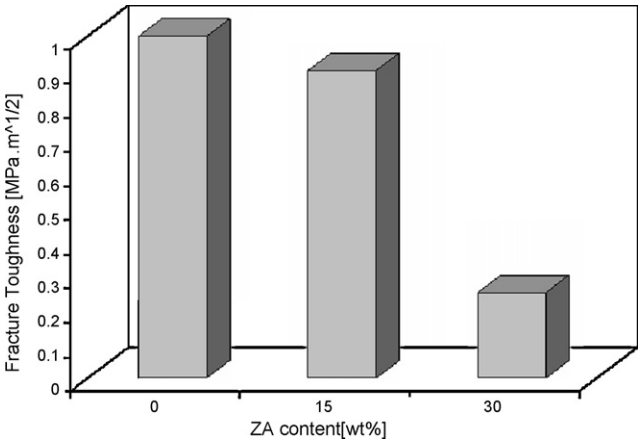

Fig. 8. Fracture toughness of the HAP-based composites containing various types of second phases at 1200 °C.

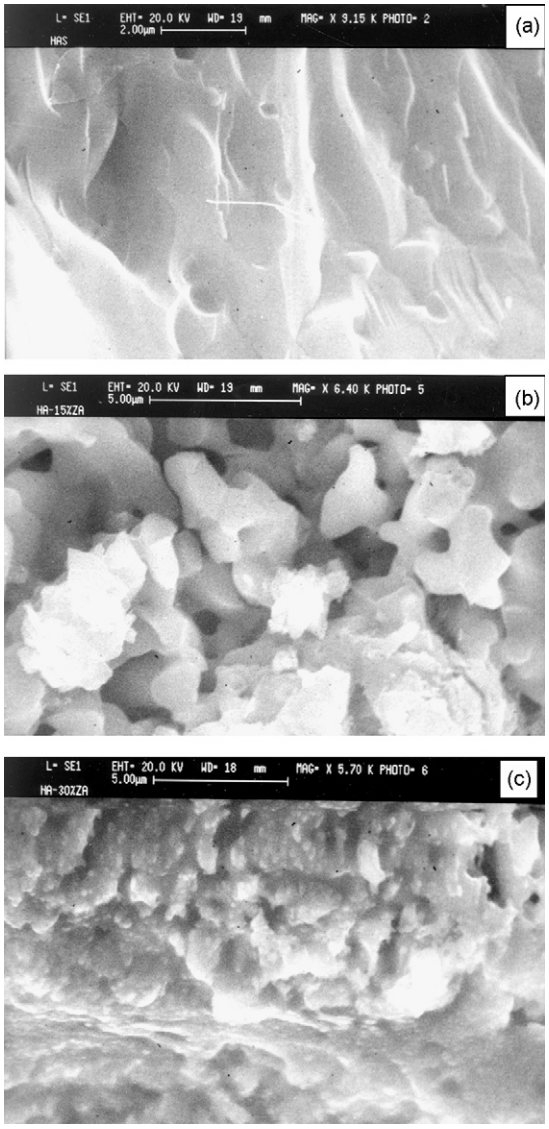

Fig. 9. SEM micrographs of fracture surfaces (a) pure HAP, (b) HAP with 15 wt% ZA and (c) HAP with 30 wt% ZA, after pressing and sintering.

As mentioned in the introduction section, ZrO_2 has high strength and toughness, but is reacts with HAP and forms TCP and water vapor. This reaction induces formation of porosity, thus reduces the strength and toughness. On the other hand, Al_2O_3 is bioinert material. Al_2O_3 can be added to ZrO_2 to reduce its negative outcomes. Thus, Al_2O_3 and ZrO_2 both affect strength and toughness of HAP composite.

SEM micrographs of the fracture surface of selected samples containing different types of second phase are shown in Fig. 9(a–c). When the pure hydroxyapatite was pressed and sintered, extensive grain growth took place and the fracture surface occurred mostly in a transgranular pattern as shown in Fig. 9(a). When 15 wt% ZA was added, the fracture morphology was changed remarkably as shown in Fig. 9(b). The fracture surfaces become very rough clearly because of the toughening effects of the reinforcing agents. The fracture surface of the specimen, prepared by 30 wt% ZA, illustrates extensive reactions between the HAP and the second phases (Fig. 9(c)) forming the TCP as confirmed by the XRD patterns (Fig. 1).

4. Conclusions

Nanocrystalline hydroxyapatite compound and alumina–zirconia composite can successfully be produced by precipitation and sol–gel techniques from starting materials. The bending strength of pressed nanocrystalline HAP was improved significantly by the addition 15 wt% of ZrO_2–Al_2O_3, but the fracture toughness was not changed. In this state the mixture colloidal processing was effective in reducing the deleterious reaction between HAP and ZrO_2. When 30 wt% of ZA powders was added to nanocrystalline HAP by the method, the bending strength and fracture toughness of the specimens decreased, because the contact area between HAP and ZrO_2 was increased.

Acknowledgment

The Corresponding author would like to acknowledge Mr. B. Nemati Akhgar for helping in preparing this paper.

References

[1] L.L. Hench, Bioceramics: from concept to clinic, J. Am. Ceram. Soc. 74 (1991) 1487.
[2] W. Suchanek, M. Yoshimura, Processing and properties of hydroxyapatite-based biomaterials for use as hard tissue replacement implants, J. Mater. Res. 13 (1.) (1998).
[3] I. Mobasherpour, M. Soulati Heshajin, A. Kazemzadeh, M. Zakeri, Synthesis of nanocrystalline hydroxyapatite by using precipitation method, J. Alloys Compd. 430 (1–2) (2007) 330–333.
[4] W.R. Rao, R.F. Boehm, A study of sintered apatites, J. Dent. Res. 53 (1974) 1351.
[5] G. De With, H.J.A. Van Dijck, N. Hattu, K. Prijs, Sintering of hydroxylapatite–zirconia composite materials, J. Mater. Sci. 16 (1981) 1592.
[6] P. Ducheyne, M. Marcolongo, E. Schepers, in: L.L. Hench, J. Wilson (Eds.), An Introduction to Bioceramic, World Scientific Publishing Co., Singapore, 1993, pp. 281–297.
[7] Y.M. Kong, S. Kim, H.E. Kim, Reinforcement of hydroxyapatite bioceramics by addition of ZrO_2 coated with Al_2O_3, J. Am. Ceram. Soc. 82 (11) (1999) 2963.

[8] D.W. Richerson, Modern Ceramic Engineering, Properties, Processing and use in Design, Marcel Decker, New York, 1992, pp. 731–807.
[9] K. Tsukuma, K. Ueda, M. Shimada, High-temperature strength and fracture toughness of Y_2O_3-partially-stabilized ZrO_2/Al_2O_3 composites, J. Am. Ceram. Soc. 68 (1.) (1985), c-4-c-5.
[10] O.N. Grigoryev, S.A. Firstov, O.A. Babiy, G.E. Homenko, Effect of zirconia (3 mol% yttria) additive on mechanical properties and structure of alumina ceramics, J. Mater. Sci. 29 (1994) 4633.
[11] S.F. Hulbert, in: L.L. Hench, J. Wilson (Eds.), An Introduction to Bioceramic, World Scientific Publishing Co., Singapore, 1993 pp. 25–40.
[12] N. Tamari, M. Mouri, I. Kondo, Mechanical properties and existing phases of composite ceramics obtained by sintering of a mixture of hydroxyapatite and zirconia, J. Ceram. Soc. Jpn. 95 (8) (1987) 806–809.
[13] J.M. Wu, T.S. Yeh, Sintering of hydroxylapatite–zirconia composite materials, J. Mater. Sci. 23 (1988) 3771.
[14] E. Champion, S. Gautier, D. Bernache-Assollant, Characterization of hot pressed Al_2O_3-platelet reinforced hydroxyapatite composites (biomaterial for orthopedics), J. Mater. Sci. Mater. Med. 7 (1996) 125.
[15] A. Mondal, S. Ram, Al^{3+}-stabilized c-ZrO_2 nanoparticles at low temperature by forced hydrolysis of dispersed metal cations in water, J. Solid State Ionics 160 (2003) 169.
[16] Y.M. Kong, C.J. Bae, S.H. Lee, H.W. Kim, H.E. Kim, Improvement in biocompatibility of ZrO_2–Al_2O_3 nano-composite by addition of HA, J. Biomater. 26 (2005) 509.
[17] B.T. Lee, C.W. Lee, M.H. Youn, H.Y. Song, Relationship between microstructure and mechanical properties of fibrous HAP-(t-ZrO_2)/Al_2O_3–(m-ZrO_2) composites, J. Mater. Sci. Eng. A 458 (1–2) (2007) 11–16.